SECURITY CLASSIFICATION OF THIS PAGE (When Data Entered)

REPORT DOCUMENTATION PAGE		READ INSTRUCTIONS BEFORE COMPLETING FORM
1. REPORT NUMBER NRL Report 7781	2. GOVT ACCESSION NO.	3. RECIPIENT'S CATALOG NUMBER
4. TITLE (and Subtitle) CORROSION OF IRON IN CREVICES		5. TYPE OF REPORT & PERIOD COVERED Final report on one phase of the NRL Problem. 6. PERFORMING ORG. REPORT NUMBER
7. AUTHOR(s) E. McCafferty		8. CONTRACT OR GRANT NUMBER(s)
9. PERFORMING ORGANIZATION NAME AND ADDRESS Naval Research Laboratory Washington, D.C. 20375		10. PROGRAM ELEMENT, PROJECT, TASK AREA & WORK UNIT NUMBERS NRL Problem M04-09; Task RR 022-08-44-5513
11. CONTROLLING OFFICE NAME AND ADDRESS Department of the Navy Office of Naval Research Arlington, Va. 22217		12. REPORT DATE August 15, 1974 13. NUMBER OF PAGES 38
14. MONITORING AGENCY NAME & ADDRESS(if different from Controlling Office)		15. SECURITY CLASS. (of this report) Unclassified 15a. DECLASSIFICATION/DOWNGRADING SCHEDULE

16. DISTRIBUTION STATEMENT (of this Report)

Approved for public release; distribution unlimited.

17. DISTRIBUTION STATEMENT (of the abstract entered in Block 20, if different from Report)

18. SUPPLEMENTARY NOTES

19. KEY WORDS (Continue on reverse side if necessary and identify by block number)

Crevice corrosion	Oxygen reduction
Iron	Chloride ion
Electrode behavior	Chromate ion
Polarization	

20. ABSTRACT (Continue on reverse side if necessary and identify by block number)

The crevice corrosion of iron has been studied in quiescent sodium chloride solutions with and without chromate inhibitor. Polarization curves have been obtained using a special device which features an adjustable crevice width and provides for measurement of electrode potential within the crevice.

(Continues)

DD FORM 1 JAN 73 1473 EDITION OF 1 NOV 65 IS OBSOLETE i
S/N 0102-014-6601

SECURITY CLASSIFICATION OF THIS PAGE (When Data Entered)

20. Abstract

In crevices where the internal iron was not short-circuited to external metal, the corrosion rate was determined by the limiting cathodic current for oxygen reduction. This limiting current, and accordingly the corrosion rate, was independent of pH and chloride ion concentration but was suppressed to a constant value when the height of the crevice was less than the thickness of the oxygen diffusion layer. When iron in the crevice was short-circuited to external, open platinum and chromate inhibitor was not used, the initial crevice corrosion rate was independent of crevice height but increased with increasing concentration of chloride ion and area of external electrode. At constant concentration of chloride ion, the crevice corrosion rate of internal iron short-circuited to open external iron decreased with increasing concentration of chromate ion. When a constant chromate-ion concentration was used which did not give protection, at short times the crevice corrosion rate was greater the greater the chloride ion concentration, but at longer times the rates were essentially independent of bulk chloride-ion concentration.

Surfaces which pitted when open did not necessarily corrode under crevices. When crevice corrosion did occur, the electrode potential within the crevice was not related to the critical pitting potential for the open sample.

CONTENTS

INTRODUCTION 1

BACKGROUND 1

EXPERIMENTAL MATERIALS AND PROCEDURE 2

Electrode 2
Crevice Assembly 3
Reference Electrodes 3
Solutions 5
Procedures 6

RESULTS AND DISCUSSION FOR INHIBITOR-FREE SOLUTIONS 7

Polarization of *Isolated* Crevices 7
Effect of Crevice Height 10
Coupled Crevices 11
Direct Short-Circuiting of Crevice and Open Metal 16
Crevice pH 17

RESULTS AND DISCUSSION FOR SOLUTIONS CONTAINING CHROMATE INHIBITOR 20

Effect of Coupling 20
Crevice Corrosion Rates 20
Potential Difference Between Inner and Outer Surfaces 25
Potential Difference and Corrosion Rate 28
Distribution of Crevice Attack 29
Comparison of Crevice Corrosion and Pitting 30

SUMMARY 33

ACKNOWLEDGMENT 34

REFERENCES 34

CORROSION OF IRON IN CREVICES

INTRODUCTION

Localized corrosion is a serious problem because the attack is highly intensified at certain areas on the metal surface, with other areas remaining unaffected. Examples include stress-corrosion cracking, pitting corrosion, and crevice corrosion. Crevice corrosion can occur between two overlapping metal sheets, within the strands of wire rope, in screw threads, or even under barnacles in a ship's hull.

In all such cases of localized attack, a special restrictive geometry forms an active "occluded corrosion cell" [1] by limiting the exchange of the bulk and local electrolytes. In the case of pitting corrosion a porous cap of corrosion products acts as the barrier; within stress-corrosion cracks and crevices the long narrow diffusion path limits the access to bulk electrolyte. The localized attack is electrochemical, but the restrictive geometry makes access to and study of the internal corroding areas difficult. Adding to the difficulty caused by this restrictive geometry is that the chemical composition of the local corrodent changes as the corrosion reaction proceeds.

The purpose of this study was to investigate the fundamental aspects of crevice corrosion in a well-defined system. Iron was chosen, partly because of the attention given this metal in a wide variety of open systems and partly to simplify composition changes in the electrolyte within the crevice. Emphasis was placed on the electrode kinetic behavior of iron confined under a flat crevice. The effect of variable crevice height, chloride ion concentration, and chromate inhibitor was considered. Some aspects of this study have been reported elsewhere [2].

BACKGROUND

Rosenfeld and Marshakov [3,4] have shown that crevice corrosion usually proceeds in two main stages as depicted in Fig. 1: initiation by differential aeration and propagation by crevice acidification. Initially the metal within the crevice is in contact with a restricted oxygen supply compared to external metal and becomes anodic relative to the external metal to which it is coupled* [5]. At longer times corrosion products accumulate within the crevice so as to change the local solution composition and pH.

Reports that not only crevices [3,4,6] but also stress-corrosion cracks [7,8] and pits [9-11] acidify locally have led to the view that all three forms of localized corrosion share the unifying feature of being "occluded corrosion cells" [1] having restricted exchange

---

Note: Manuscript submitted June 6, 1974

*This follows from application of the Nernst equation, namely, $E = E^{o} - (RT/nF\ell n([\text{products}]/[\text{reactants}])$, to the oxygen reduction reaction: $0_2 + 2H_20 + 4e^{-} \rightarrow 40H^{-}$. The electrode in contact with the smaller oxygen concentration will have the less positive electrode potential (anode upon coupling).

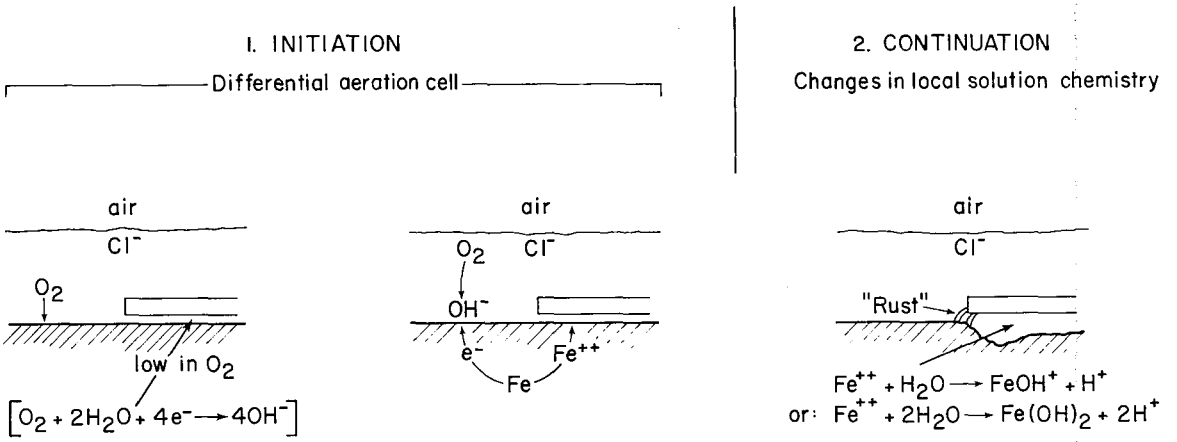

Fig. 1 — Progression of crevice corrosion

with bulk electrolyte and thus have common solution chemistries. Hence most recent studies have used the thermodynamic rather than kinetic approach, with emphasis on factors such as resultant crevice solution chemistry, pH, and electrode potential [12-15]. Little recent work has been done on the electrode kinetic behavior of metals under crevices. One exception has been the correlation between the shape of cyclic anodic polarization curves for various engineering alloys in 3-1/2% NaCl with their longer range performances in natural seawater [16]. Polarization curves have been reported in some well-defined but synthetic, generalized "occluded corrosion cells" *sans* crevices, in which the "internal" metal was activated by anodic polarization [17] or by deaeration [18]. Other investigators have reported current-vs-time [19] and potential-vs-time [14,20], but not current-vs-potential relationships.

The purpose in this study therefore was to take up the systematic method of Rosenfeld and Marshakov [3] in order to investigate in an organized manner the kinetic aspects of a model crevice.

EXPERIMENTAL MATERIALS AND PROCEDURE

Electrode

Ferrovac E high-purity iron (Table 1) was used in this study. An iron electrode (3.18 cm in diameter) was encased in a Teflon holder by pressing the cylindrical iron bar through an undersized opening in the Teflon. The uppermost rim of Teflon was machined away, and the electrode edge was masked with alkyd varnish, a material found suitable in preventing the formation of unintentional, microscopic crevices [21]. Before use, the exposed iron face (7.9 cm^2 projected area) was dry-polished through 3/0 emery papers, washed with ethanol, and dried in a stream of nitrogen.

Table 1
Analysis of Ferrovac E
High-Purity Iron

Impurity	Content (%)
C	0.007
Mn	0.01
P	0.002
S	0.007
Si	0.006
Ni	0.025
Cr	0.007
V	<0.01
W	0.02
Mo	<0.01
Cn	<0.001
Co	0.01

Crevice Assembly

The electrode holder was machined to fit into the cell as shown in Fig. 2. The assembled device is shown in Fig. 3. A central feature of the assembly is the adjustable crevice height. The crevice was formed by positioning the optically polished bottom surface of a glass disk a measured distance from the iron surface by means of a micrometer attached to the disk top. Two small holes (<1 mm in diameter) through the glass disk led to Ag/AgCl reference electrodes. These Luggin capillaries enabled measurement of the electrode potential at two locations in the crevice: the center and near the edge. Thus electrochemical processes *within* the crevice could be monitored.

Reference Electrodes

The Ag/AgCl electrodes were prepared by anodizing Ag wire in 0.1N HCl for 30 minutes at a current density of 0.4 mA/cm^2 [22]. The electrodes to be located at the two locations within the crevice were always checked against each other before use. The solution in the capillary section was the same as the bulk electrolyte and was kept from draining into the crevice by filter-paper plugs packed into the capillary bottom. Electrode potentials were thus measured versus Ag/AgCl in the test solution but were converted to potentials versus a standard Ag/AgCl reference electrode housed in the usual mixture of KCl (4M) and AgCl (saturated). These conversions were made using the data in Fig. 4, which shows that the potential of the chlorodized silver wire depended primarily on the Cl^- concentration. For example, with $[CrO_4^{=}] \leqslant 0.006N$,*

*Normalities of $CrO_4^{=}$ are given in terms of 2 equivalents/mole.

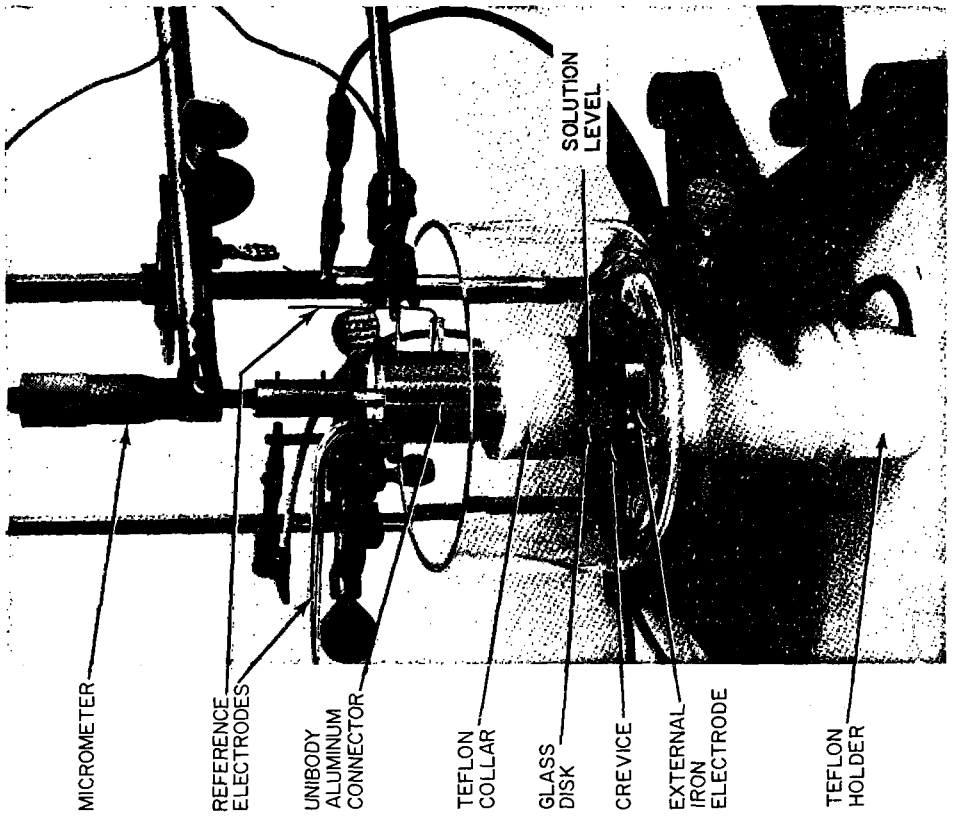

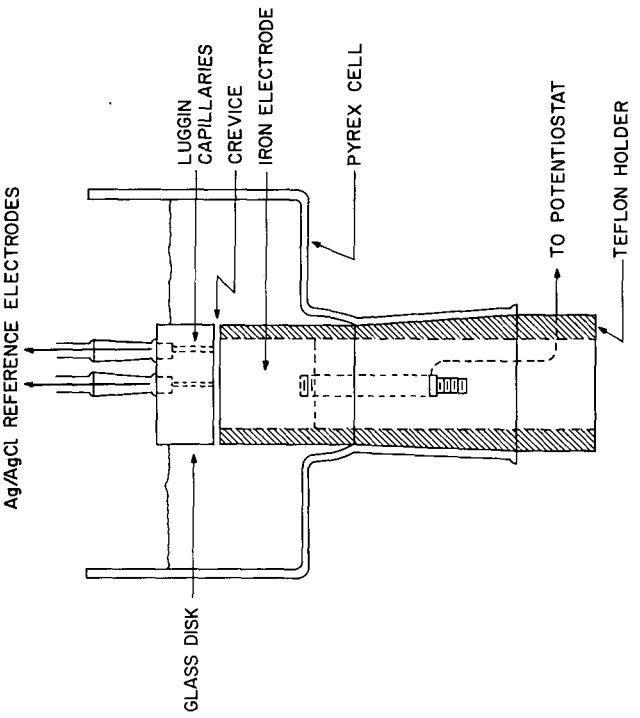

Fig. 2 — The crevice corrosion cell. (The micrometer assembly and auxiliary electrode are not shown.)

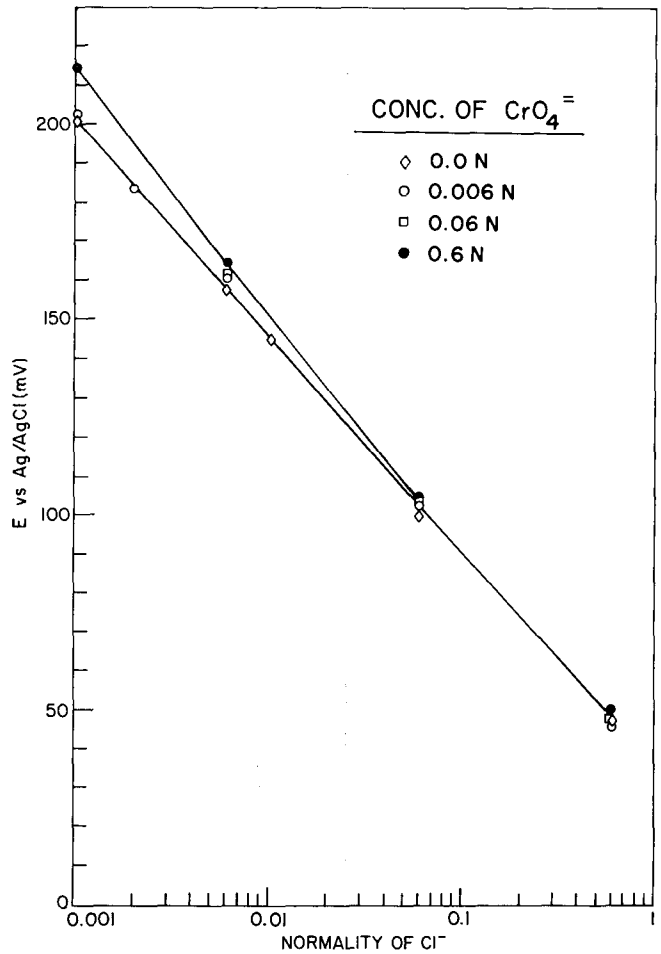

Fig. 4 — Potential of chlorodized silver wire in various $Cl^-/CrO_4^=$ solutions

$$\left(\frac{\partial E}{\partial \log [Cl^-]}\right)_{[CrO_4^=]} = 55 \text{ mV} \tag{1}$$

compared to the theoretical value of 59 mV (based on activities rather than concentrations). For the more dilute Cl^- concentrations, there was a slight dependence of measured potential on the $CrO_4^=$ concentration, but the appropriate corrections were made for each solution used.

Solutions

Sodium chloride solutions were used:

- with sodium chromate inhibitor (pH = 8.4), to study the crevice corrosion of passive iron,

- without inhibitor (pH = 5.5), to study active crevices.

The 3-1/2% NaCl solution (wt/vol) was of particular interest because the Cl^- concentration (0.6N) is the same as in natural seawater. All solutions were prepared from reagent grade chemicals and double-distilled water prepared in a quartz still. During all experiments the cell electrolyte was open to the air and unstirred.

Procedures

For the $CrO_4^=/Cl^-$ solutions an iron ring (area $\approx$ 50 cm^2) cut from the same bar as the crevice iron was used as the external open electrode. This split-electrode arrangement allowed measurement of current between active internal and passive external electrodes. After 15 minutes immersion in a given solution, the two parts were short-circuited through a Wenking potentiostat used in a two-electrode configuration [23] (Fig. 5). This arrangement essentially uses the potentiostat as a zero-resistance ammeter and short-circuits the two electrodes by setting a zero potential difference between them. Electrode potentials of internal iron and crevice iron were measured on the same digital electrometer (Keithley 615). The $CrO_4^=$ and Cl^- concentrations were varied, but the crevice height was fixed at 10 mils (0.25 mm) for this set of experiments.

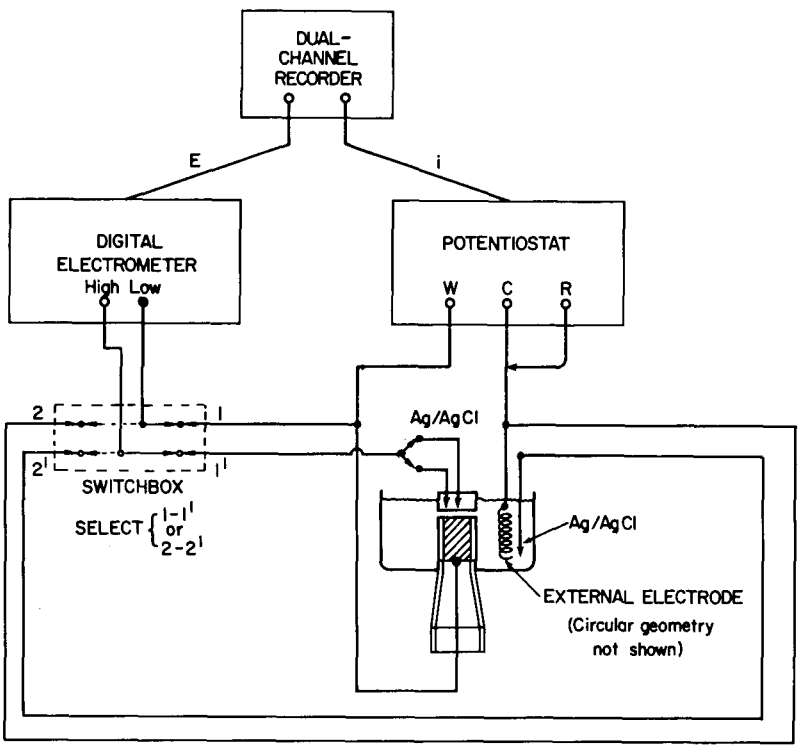

Fig. 5 — Schematic diagram of the experimental set up

Two types of crevices were investigated for the chromate-free solutions:

- *isolated* crevices, in which internal iron was not connected to external metal, and
- *coupled* crevices, in which internal iron was short-circuited to external metal.

The former configuration allowed study of local cell activity within a crevice, and the latter simulated the more practical case in an overlapping joint, for example, where metal within the crevice is in electrical contact with metal outside the crevice.

The effect of crevice width, pH, and Cl^- concentration was studied for the *isolated* crevice. The narrower *isolated* crevices were polarized galvanostatically using a number of variable resistors in series with a 45-V battery ($R_{ext} >> R_{cell}$). (Use of the potentiostat in the normal three-electrode configuration yielded oscillations in current for the narrower crevices, but there were no problems with thicker crevices or with the two-electrode configuration for *coupled* crevices.)

For *coupled* crevices in the chromate-free solutions, a platinum gauze electrode was used as the open, external electrode in order to confine corrosion to the internal iron. Crevice iron and external platinum were immersed (uncoupled) for 24 hours to reach steady-state potentials prior to coupling through the potentiostat in the two-electrode configuration. Evans polarization diagrams were determined for different crevice heights, Cl^- concentrations, and external areas.

RESULTS AND DISCUSSION FOR INHIBITOR-FREE SOLUTIONS

Polarization of *Isolated* Crevices

Polarization curves were determined after 24 hours immersion in 0.6N and 0.06N NaCl solutions. Steady-state open-circuit potentials were established in about 10 hours (Fig. 6). In all cases open-circuit potentials measured at the crevice center were identical with potentials measured near the crevice edge.

Figure 7 shows typical polarization curves in 0.6N NaCl for both the open sample and for *isolated* crevices (crevice metal not coupled to open external metal). In all cases the cathodic branch was determined first, open circuit was reestablished, and the anodic branch was then determined. For cathodic polarization, electrode potentials measured via the Luggin capillary at the crevice center were the same as those near the edge. For anodic polarization, in a few cases there were slight differences between the two locations (5 to 20 mV), but only at high anodic overvoltages.

The shape of the cathodic curves in Fig. 7 is characteristic of a diffusion-controlled process. The overall cathodic reaction in nearly neutral solutions is the reduction of oxygen [24]:

$$O_2 + 2H_2O + 4e^- \rightarrow 4OH^-. \qquad (2)$$

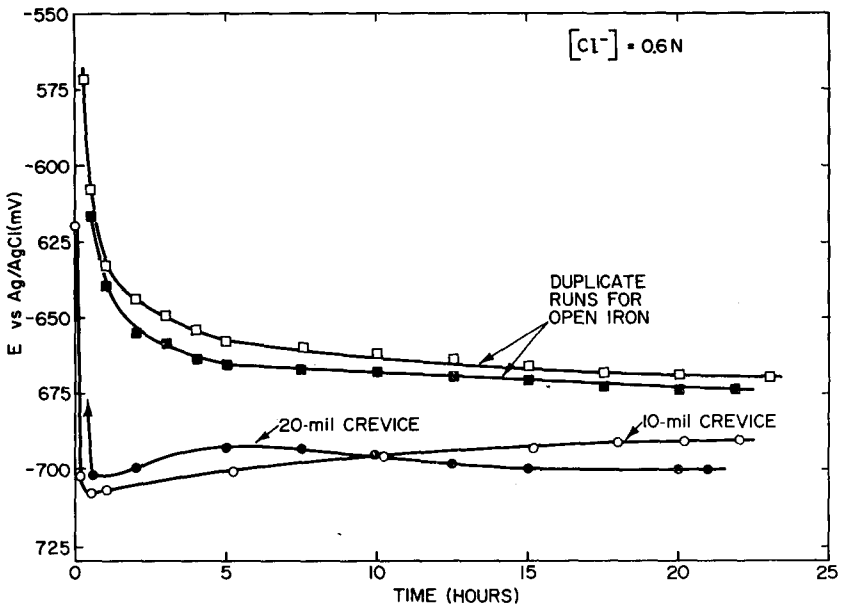

Fig. 6 — Establishment of steady-state open-circuit potentials for open iron and crevice iron in 0.6N NaCl

The anodic branches are activation controlled, with Tafel slopes of 40 to 60 mV/decade. All anodic curves were well behaved, and none displayed the peculiar property observed by Rosenfeld and Marshakov [3,4], in which some anodic curves started out in the direction of more negative potentials before turning back toward more positive potentials.

For both the crevices and the open sample the corrosion rate at open-circuit potential is equal to the limiting cathodic current for oxygen reduction, according to

$$i_{net} = i_{Fe} + i_{O_2} = 0. \tag{3}$$

With these *isolated* crevices the limiting cathodic current density for oxygen reduction is less than that for the open sample, and correspondingly so is the iron corrosion rate (Fig. 7). This same effect has been seen by Rosenfeld and Marshakov [3,4].

At more negative potentials than in Fig. 7 the predominant cathodic reaction is hydrogen evolution [25],

$$4H_2O + 4e^- \rightarrow 4OH^- + 2H_2 \text{ (gas)}, \tag{4}$$

rather than oxygen reduction. With extensive cathodic polarization the shape of the polarization curve changed from diffusion control to activation control and exhibited a Tafel slope of 120 mV/decade, characteristic of hydrogen evolution [26]. Figure 8 shows the change in shape of the cathodic polarization curve with extensive cathodic polarization (20-mil crevice; 0.06N NaCl). In the oxygen reduction region the polarization behavior

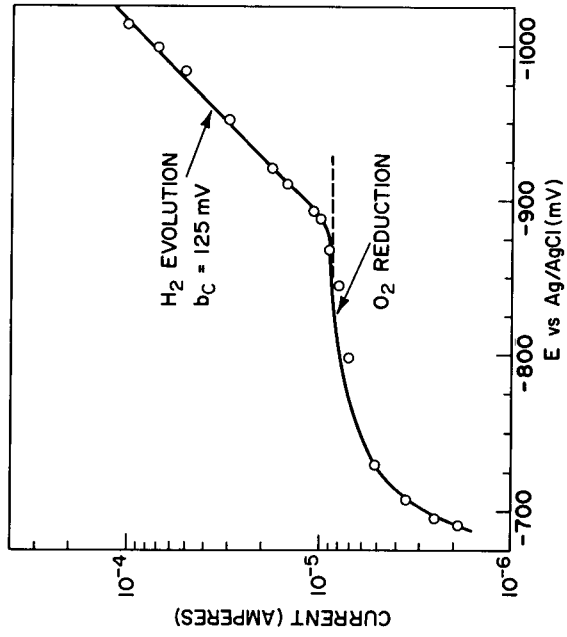

Fig. 8 — Change in shape of the polarization curve for iron at high cathodic overvoltages: 20-mil crevice (0.51 mm.) in 0.06N NaCl

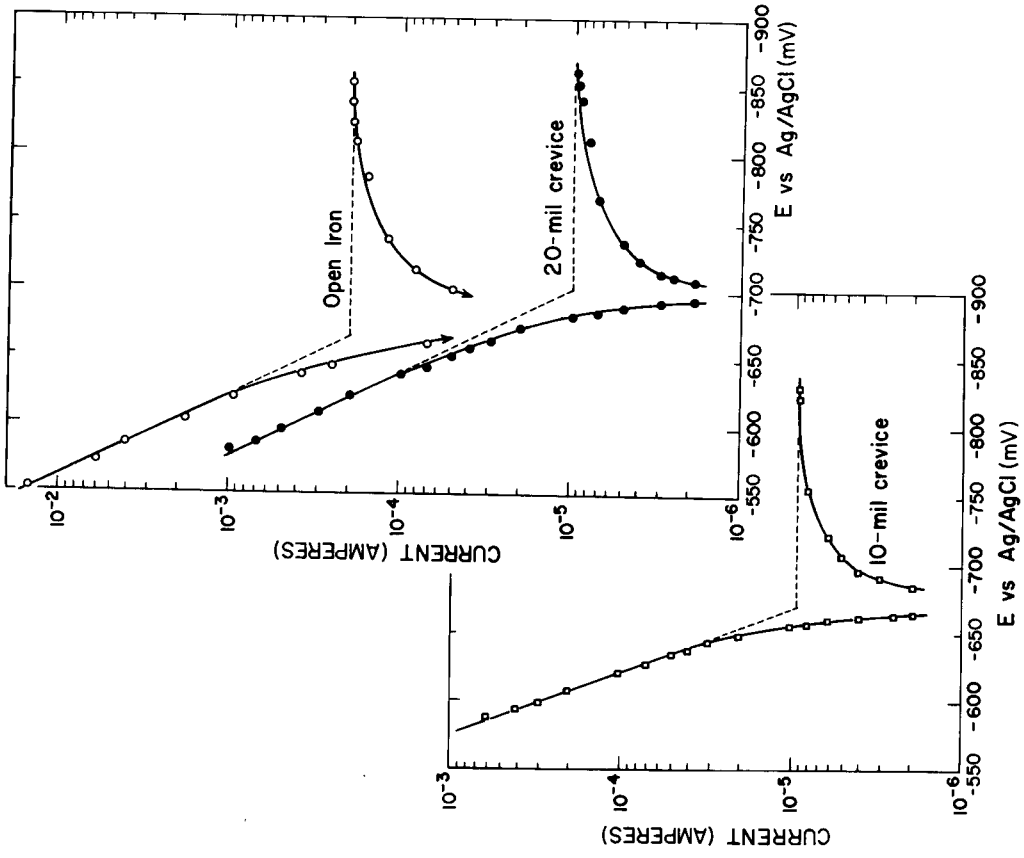

Fig. 7 — Polarization curves for open iron and iron in *isolated* crevices in 0.6N NaCl after 24 hours immersion

was independent of pH and Cl^- ion concentration, as required by Eq. (3); this is shown in Fig. 9 for a 10-mil crevice.

Effect of Crevice Height

The effect of the *isolated* crevice is thus to stifle the oxygen reduction reaction, even for a relatively wide opening of 125 mils (3.18 mm), as seen in Fig. 10 for 0.06N NaCl. The limiting cathodic rate is further suppressed to a constant value for crevice heights from 5 to 20 mils (0.13 to 0.51 mm). The crevice height of 20 mils (0.51 mm) is significant in that it is approximately the thickness δ of the oxygen diffusion layer near the electrode surface calculated [27] from

$$i_{l,c} = nF \frac{D}{\delta} C, \tag{5}$$

where $i_{l,c}$ is the mass-transfer limited cathodic current density for the open sample (0.20 mA/7.9 cm^2), n = 4 electrons transferred per mole O_2 according to Eq. (2), and D and C are the diffusion coefficient and concentration respectively of oxygen. With D = 1.65 X 10^{-5} cm^2/s [28] for 0.05N NaCl at 25°C and C = 8.2 mg/l [29], Eq. (5) gives δ = 0.063 cm or 25 mils. This value agrees with that of Rosenfeld and Vashkov [30], who calculated the thickness of the diffusion layer to be 0.50 mm (20 mils) for iron in 0.5N NaCl. Experiments by Rosenfeld and Marshakov [4] with variable crevices gave δ = 0.25 to 0.50 mm.

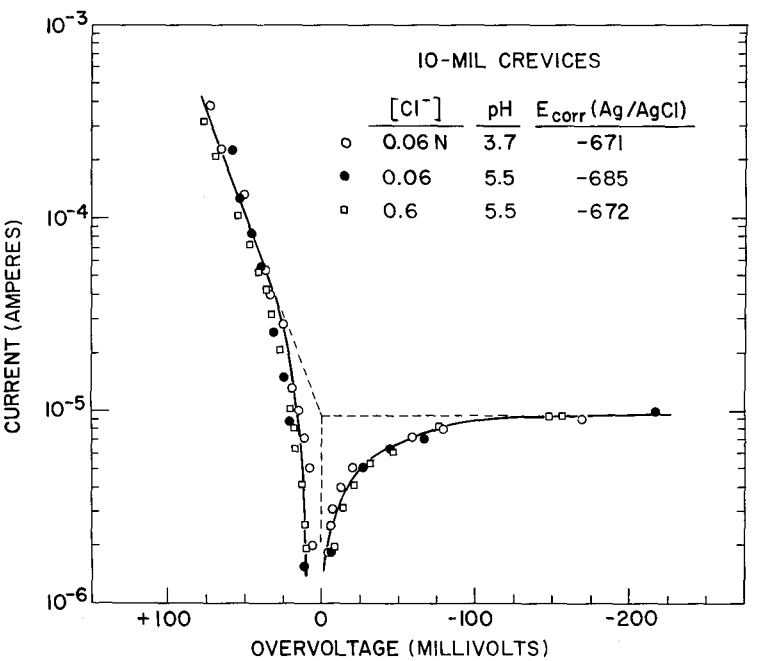

Fig. 9 — Effect of pH and Cl^- ion concentration on the polarization of iron in 10-mil (0.25-mm) *isolated* crevices

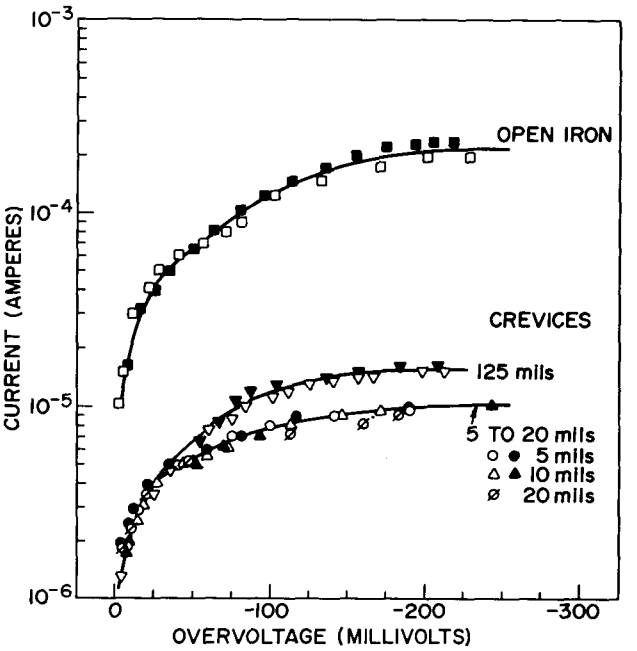

Fig. 10 — Effect of crevice height on the cathodic polarization of iron in 0.06N NaCl. (Duplicate runs are indicated by open and solid symbols.)

Thus in crevices not coupled to outside open metal, when the crevice height is comparable to or less than the thickness of the oxygen diffusion layer, diffusion of oxygen into the crevice is impeded and hence the corrosion rate is reduced, according to Eq. (3).

All polarization curves reported were steady-state curves. Figure 11 shows potential-vs-time dependence for the galvanostatic cathodic polarization of a 20-mil crevice in 0.06N NaCl. For the lowest applied currents, only a few minutes were necessary to establish a steady potential, but several hours were necessary to reach a steady potential near the limiting cathodic current for oxygen reduction.

Coupled Crevices

The effect of activating the crevice iron was studied by coupling it to external, open platinum. This arrangement simulates practical cases, such as in an overlapping joint, where metal within the crevice is in electrical contact with passive metal outside the crevice. The iron in the crevice was connected to the external platinum gauze using the potentiostat in the two-electrode configuration [23] shown in Fig. 5. This arrangement forces the cathodic reaction (oxygen reduction) to continue outside the crevice at the platinum surface after the oxygen within the crevice has been consumed. Thus the anodic reaction (iron dissolution) is confined to the crevice.

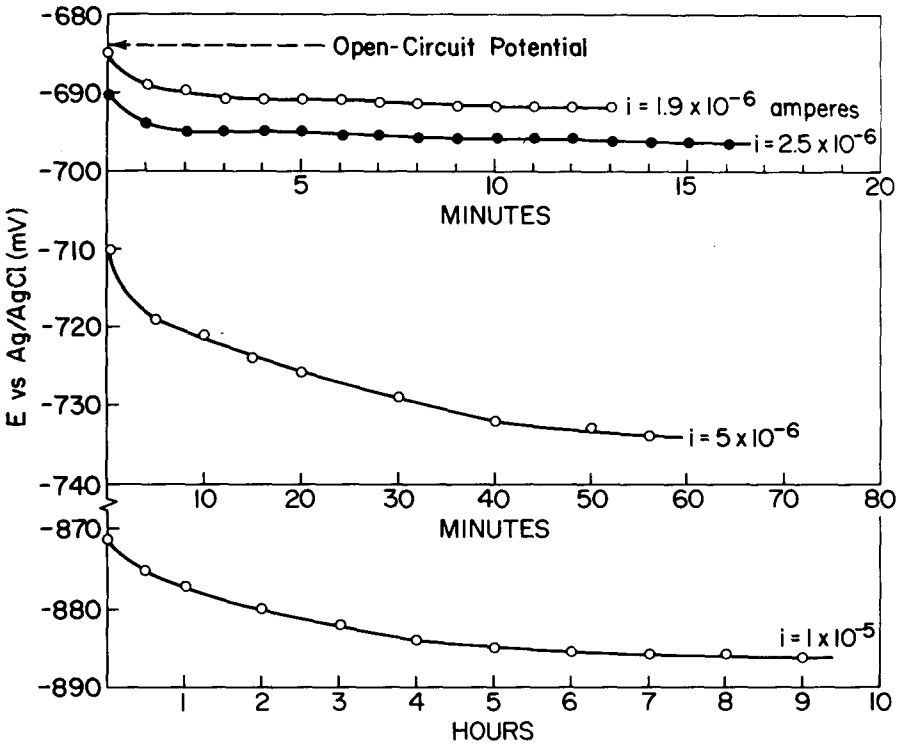

Fig. 11 — Establishment of equilibrium potentials during the galvanostatic polarization of iron in a 20-mil (0.51-mm) crevice in 0.06N NaCl

Evans polarization diagrams are shown in Fig. 12 for 0.06N NaCl. Initially the iron and platinum were uncoupled for 24 hours so that each electrode reached its own steady potential. These open-circuit potentials for uncoupled iron and uncoupled platinum tend toward the bottom of the diagram (toward zero current flow). A fixed *potential difference* was set between the inner iron and outer platinum. Within 5 to 20 minutes there resulted a constant current and steady *electrode potentials* for the crevice iron and open platinum. Those are the points plotted in Fig. 12. With increased current flow between the iron crevice and open platinum, the two electrode potentials approached each other. At the point of direct-coupling (zero set potential difference) there was an IR drop between the crevice center and the open outer electrode. However this IR drop at the point of direct coupling occurs on the flat portion of the oxygen-reduction curve for platinum. Thus the corrosion current for the short-circuited couple is essentially given by the intersection of the anodic and cathodic polarization curves.

In all cases, the short-circuited corrosion current became steady after 5 to 20 min. Longer range behavior was not followed in this set of experiments.

Table 2 lists the value of the IR drops for the various experiments. With 0.6N NaCl the IR drop was about 50 mV. For 0.06N NaCl the IR drop increased from 20 mV for the open sample to nearly 200 mV for the thinnest crevice studied (3 mils).

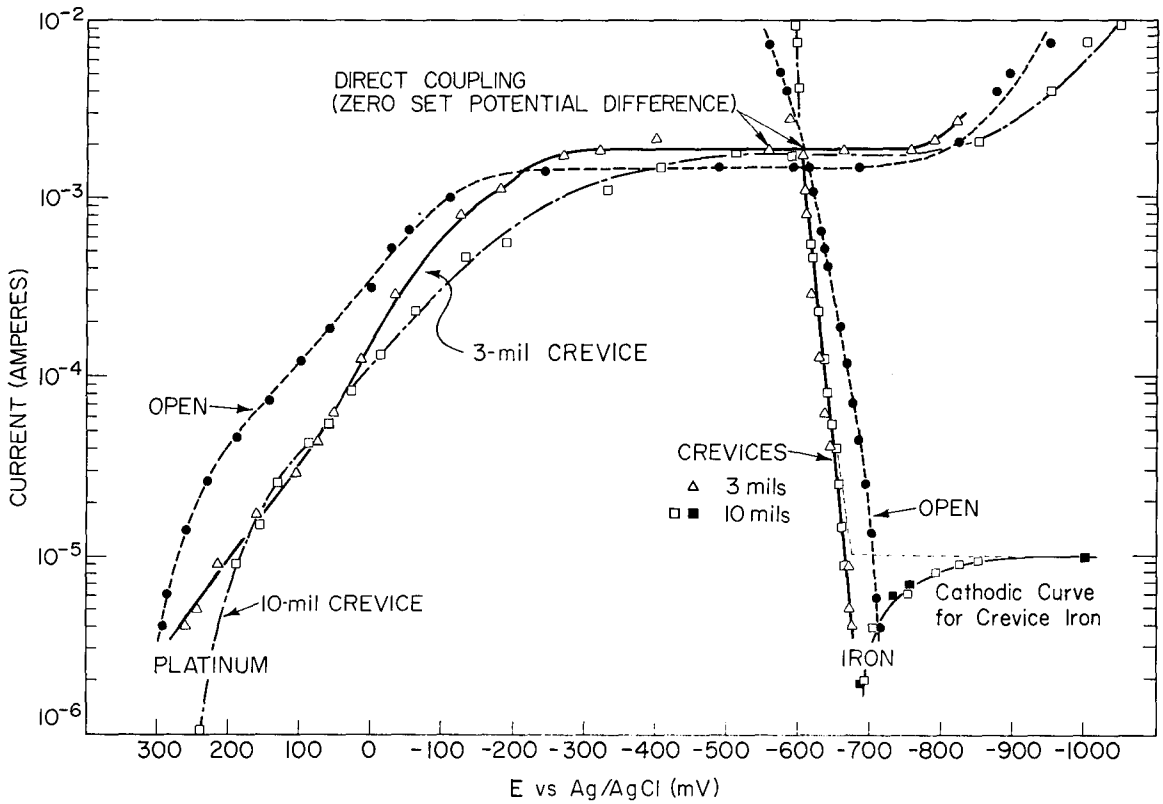

Fig. 12 — Evans polarization diagrams for iron coupled to platinum in 0.06N NaCl. (Duplicate runs for 10-mil crevices are indicated by open and solid squares.)

Figure 12 shows that the short-circuit corrosion current for the crevices is increased slightly compared to the value for the open sample (1.8 mA vs 1.5 mA respectively). Thus even a crevice as narrow as 3 to 10 mils does not hinder the corrosion of iron in the crevice once the iron has been activated by coupling to an external cathode. However the attack is concentrated near the crevice edge.

As was found for the *isolated* crevices, the electrode potentials of iron at the crevice center and near the crevice edge were either identical or displayed only small differences (5 to 15 mV).

Figure 12 also compares the crevice corrosion current for the *isolated* (uncoupled) crevices to that for the iron/platinum couples. In the former case the crevice corrosion current is only 1×10^{-5} amps (Fig. 9) and is determined by the rate of oxygen reduction *within* the crevice. As seen in Fig. 12, the corrosion rate of the coupled crevices is also under cathodic control. Here however the corrosion rate is determined by the rate of oxygen reduction at the open electrode *outside* the crevice.

Table 2
IR Drop Between the Crevice Center and External Platinum (Gauze) Electrode When Coupled

Height of the Crevice Opening (mils)	Run No.	E vs Ag/AgCl (mV)		IR Drop (mV)
		Crevice Fe	Open Pt	
0.06N NaCl				
3	30	−593	−398	195
10	27	−608	−510	98
	29	−617	−460	157
∞	28	−611	−590	21
0.6N NaCl				
10	41	−579	−537	42
	42	−581	−528	53
	45	−588	−539	49
20	44	−592	−541	51

Figure 13 shows the effect of the bulk Cl^- concentration and of external cathode area on the polarization behavior of the couple iron (crevice)/platinum (open). The results of the various experiments are summarized in Tables 3a and 3b.

Figure 13 and Table 3a show that for a given crevice height and chloride content an increase in area of the external cathode causes an increase in crevice corrosion current. The ratio of open to sheltered metal has been shown to be important in longer range, more practical immersion tests. For example, Ellis and LaQue [31] have reported a linear increase in weight loss with increasing external area for stainless steel in flowing seawater.

Table 3a also shows that increasing the bulk concentration of chloride ion increases the corrosion current for a given external area and crevice height. However a change in crevice height for a given external area and chloride content (either 0.06N or 0.6N) has no effect on the crevice corrosion rate. The explanation may be that the concentration of chloride ions entering the crevice is not strongly dependent on the crevice height. Work by Ulanovskii and Korovin [32,33] has shown that the increase in Cl^- concentration during the anodic polarization of graphite is about the same for 0.2-mm (8-mil) as for 0.6-mm (24-mil) crevices.

Table 3a also shows that the measured crevice corrosion current was not affected by variations in the experimental procedure. With 0.6N NaCl the short-circuit current was

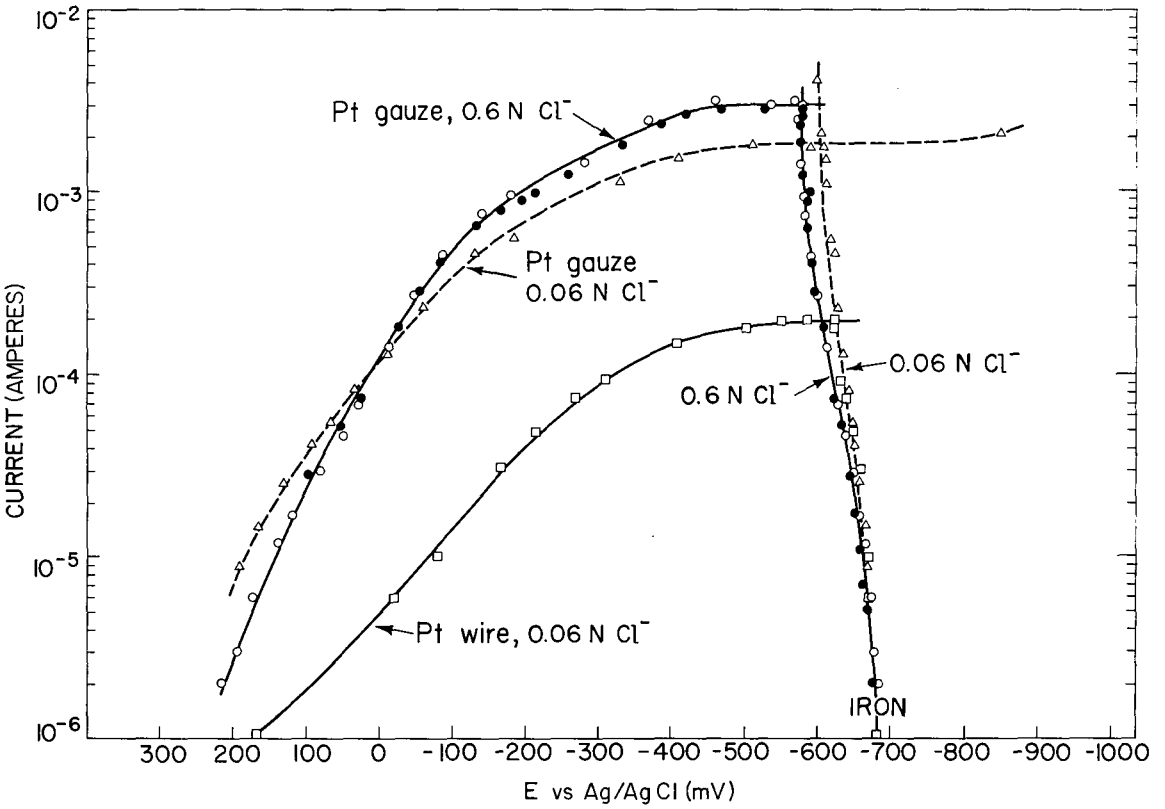

Fig. 13 — Effect of Cl^- ion concentration and area of external platinum on the polarization behavior of the couple iron (10-mil crevice)/platinum (open). (Duplicate runs are indicated by open and solid circles.)

Table 3a
Short-Circuit Current for Iron Coupled to Platinum

Cl^- Conc.	External Cathode		Short-Circuit Current (mA)			
	Type	Approx. Area (cm^2)	3-mil Crevice	10-mil Crevice	20-mil Crevice	Open Iron
0.06N	Wires	3	—	0.20	—	0.17
	Gauze	175	2.1	1.8, 2.1	—	1.5
0.6N	Gauze	175	—	2.9, 2.8, 2.5*	3.2†, 3.0	—

*Horizontally positioned platinum cathode.
†Galvanostatic run.

Table 3b
Effect of Various Parameters on the
Short-Circuit Current i_{sc}

Parameter Increased	Effect on i_{sc}
Crevice height	None
Cl^- concentration	Increase
Area of external electrode	Increase

the same for galvanostatic polarization as for potentiostatic polarization. Also it made no difference if the platinum external electrode were positioned horizontally or vertically (same area in each case).

Direct Short-Circuiting of Crevice and Open Metal

In additional experiments crevice iron and open platinum were short-circuited directly with a copper wire instead of using the potentiostat in the usual two-electrode mode (as a zero-resistance ammeter). Figure 14 shows the electrode potential behavior of iron in a 10-mil crevice when short-circuited directly to open platinum in 0.06N NaCl. After 3 hours of coupling the electrode potentials of the two components were constant. Values were: E(crevice Fe) = −621 mV vs Ag/AgCl, and E(open Pt) = −520 mV. These values compare well with those obtained for the potentiostatic experiment for the same system: −617 and −460 mV respectively. Data for various experiments in which the two methods were compared are listed in Table 4. Agreement is quite good: variation between the two methods is about the same as variations in the coupled potentials for repeat runs with the polarization technique.

In a few experiments the crevice corrosion current for the direct short circuit was measured using a simple zero-resistance ammeter [34] shown schematically in Fig. 15. As shown in Table 4, results were in good agreement with the potentiostatic results.

Thus the potentiostatic method, in which inner and outer electrodes are eventually short-circuited after a series of potential steps, gives the same results as immediate and direct short-circuiting. The potentiostatic technique has the advantages of (a) giving information on the kinetic behavior of each member of the couple and (b) giving the short-circuit current directly, without the need of balancing a galvanometer.

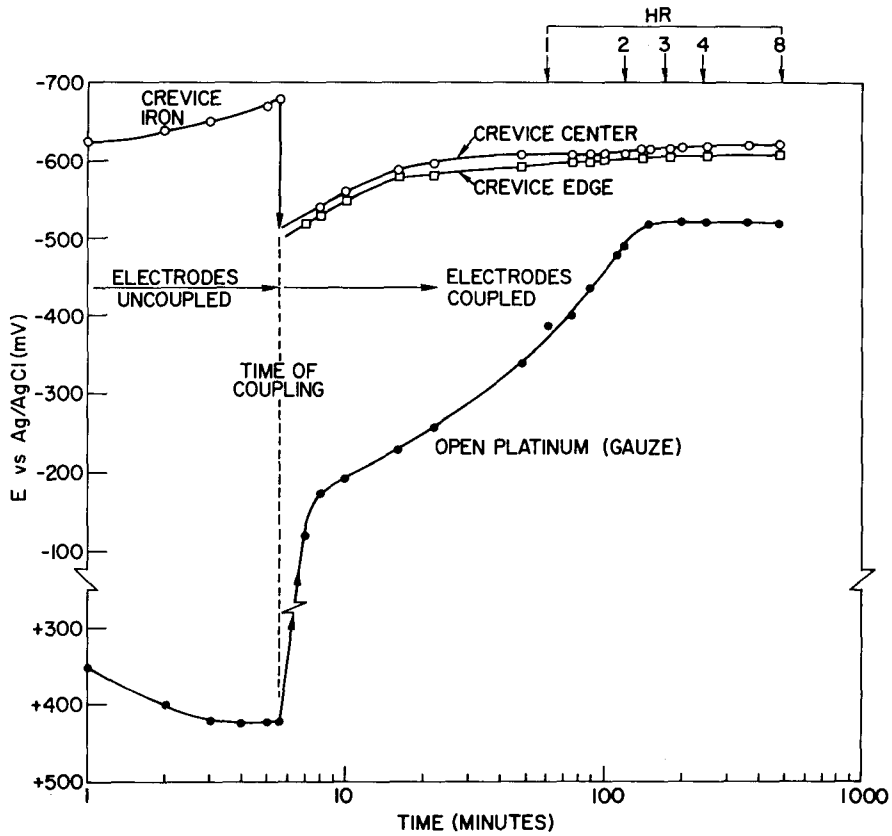

Fig. 14 -- Electrode potential behavior of crevice iron and open platinum before and after coupling (run 29; 10-mil crevice)

Crevice pH

The average pH within the crevice was measured after completion of each potentiostatic experiment with 0.06N NaCl. Bulk electrolyte from the cell was slowly pipetted off below the crevice level, and the crevice was opened carefully. A thin slurry of electrolyte plus corrosion products remained on the iron surface. The average pH of the crevice was measured either by touching a micro-pH electrode to this thin layer or by using narrow-range pH papers. Results are given in Table 5. The average crevice pH for crevice iron in 0.06N NaCl was 4.7 ± 0.3. The initial pH of the bulk solution was 5.5, but the final pH was higher (6.5 to 8.5) due to production of hydroxyl ions at the outer electrode by the reduction of oxygen:

$$O_2 + 2H_2O + 4e^- \rightarrow 4OH^-. \qquad (2)$$

The crevice pH of 4.7 for iron in 0.06N NaCl is the same value as measured for iron crevices in 0.6N NaCl by Bogar [13], who sampled crevice electrolytes with a micro-capillary and touched the extracted drops to narrow-range pH papers. Pourbaix [10] predicted the pH within an iron corrosion pit to be 4.8, assuming that at equilibrium the pit contents are a mixture of Fe, Fe_3O_4, and $Fe\ Cl_2 \cdot 4H_2O$ in the presence of an electroneutral solution.

Table 4
Comparison of Results From the Direct-Short-Circuit and Potentiostatic-Polarization Methods for Iron Crevices in 0.06N NaCl

Height of the Crevice Opening (mils)	Run No.	E vs Ag/Ag Cl (mV)			Short-Circuit Current (mA)
		Crevice Fe	Open Pt		
			Gauze	Wire	
Direct Short Circuit (Current Measured With a Zero-Resistance Ammeter)					
3	30	−619	−380	—	2.1
10	26	−615	−480	—	—
	27	−610	−440	—	—
	29	−621	−520	—	—
	26	−639	—	−626	0.16
	27	−637	—	−620	0.20
Potentiostatic Polarization (Current Measured With the Potentiostat in the Two-Electrode Configuration)					
3	30	−593	−398	—	2.1
10	27	−608	−510	—	1.8
	29	−617	−460	—	2.1
	31	−617	—	−580	0.20

An accumulation of ferrous ions within the crevice has been found [6,16] to accompany the low pH. Possible equilibrium reactions leading to an increase locally in H^+ ions have been summarized in Ref. 6. These reactions involve the hydrolysis of ferrous ions entrapped within the crevice:

$$Fe^{++} + H_2O \rightarrow FeOH^+ + H^+ \tag{6}$$

or

$$Fe^{++} + 2H_2O \rightarrow Fe(OH)_2 + 2H^+. \tag{7}$$

Detailed step-by-step mechanisms for dissolution within crevices have not been determined. However Fig. 13 does show that in the early stages of the corrosion process the Cl^- ion does not stimulate the anodic reaction. At constant potential (and constant pH = 4.7, in view of the preceding paragraph), the anodic rate is lower for the higher Cl^- concentration, in agreement with results for open iron in deaerated systems [35,36].

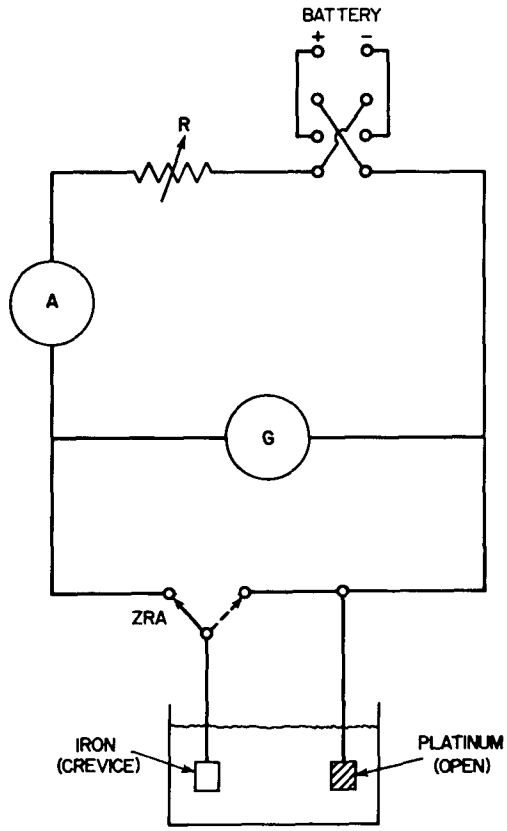

Fig. 15 — Zero resistance ammeter (ZRA)

Table 5
Measured pH Within Iron Crevices After
Polarization in 0.06N NaCl

Crevice Height (mils)	Run No.	Outer Electrode	Measured Crevice pH	Technique
3	30	Pt gauze	4.5 to 5.0	pH papers; microelectrode
10	27	Pt gauze	4.6	pH papers
	29	Pt gauze	4.6	pH papers
	31	Pt wire	4.5 4.7	Microelectrode pH papers
Range of Crevice pH Initial pH of Bulk Solution Final pH of Bulk Solution			4.7 ± 0.3 5.5 6.5 to 8.7	

RESULTS AND DISCUSSION FOR SOLUTIONS CONTAINING CHROMATE INHIBITOR

Sodium chromate was added to the chloride solutions to study the crevice corrosion of iron initially passive. In these experiments the outer electrode was the disk of iron cut from the same bar as the crevice iron sample. These experiments also investigated the longer term behavior of the couple iron(internal)/iron(external), though it is recognized that the duration of the experiment is decidedly less than the time of practical immersion tests with commercial alloys.

Effect of Coupling

Results for a typical experiment in which iron within the crevice (7.9-cm^2 area) was coupled to open, external iron ($\approx$50-cm^2 area) are shown in Fig. 16a. For the first 15 minutes the crevice iron and external iron were uncoupled (each at its own open-circuit potential). At 15 minutes the electrodes were short-circuited by using the potentiostat in the two-electrode configuration. Upon coupling, the potentials of the crevice iron and external iron shifted toward each other but were not identical due to an IR drop between the crevice interior and the outer electrode. In all experiments the initial shift in potential upon coupling was larger for the crevice iron than for external iron. At the end of the experiment shown in Fig. 16a (48 hours) the potential difference between crevice iron (laden with corrosion products) and passive external iron was only 7 mV. The maximum potential difference for this experiment was 34 mV at 30 minutes.

Figure 16a shows that there was no difference in electrode potential between the crevice center and crevice edge before coupling. After coupling, the potential of the crevice edge was usually intermediate to that of the crevice center and external iron. But at the end of every experiment there again was no difference in potential between the two locations in the crevice.

Results for two additional chloride concentrations are shown in Figs. 16b and 16c. The general appearance of these curves is similar to those in Fig. 16a.

Crevice Corrosion Rates

Figures 16 also show the crevice corrosion current between inner and outer iron surfaces when coupled. In each case the current reached a maximum and then gradually decreased with time.

The decrease in crevice corrosion current with time is due to changes in the composition of the internal crevice electrolyte. First, as the crevice iron becomes active, the accumulation of ferrous ions within the crevice causes a decrease in local pH, as discussed earlier. (For all cases except 0.6N Cl^-/0.6N $CrO_4^=$, where there was little crevice corrosion, the measured crevice pH after 48 hours was in the range 4.5 to 6.0, as compared to the bulk pH of 8.4.) In going from neutral to acidic solutions the anodic polarization curve for active iron is shifted to *lower* current density values at constant potential for

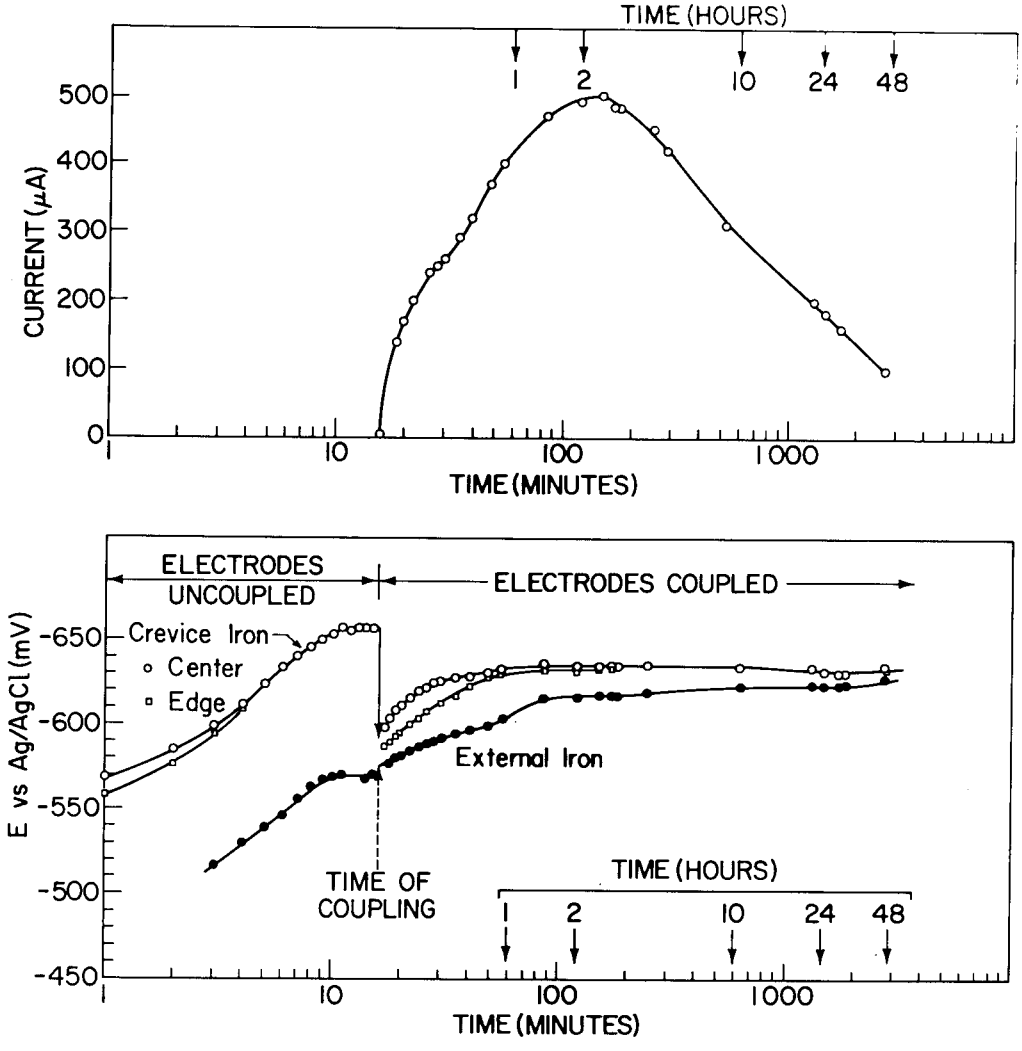

Fig. 16a — Effect of coupling iron within a 10-mil (0.25-mm) crevice in 0.006N Na_2CrO_4 + 0.6N NaCl to open external iron (area of crevice iron = 7.9 cm^2; area of external iron = 50 cm^2)

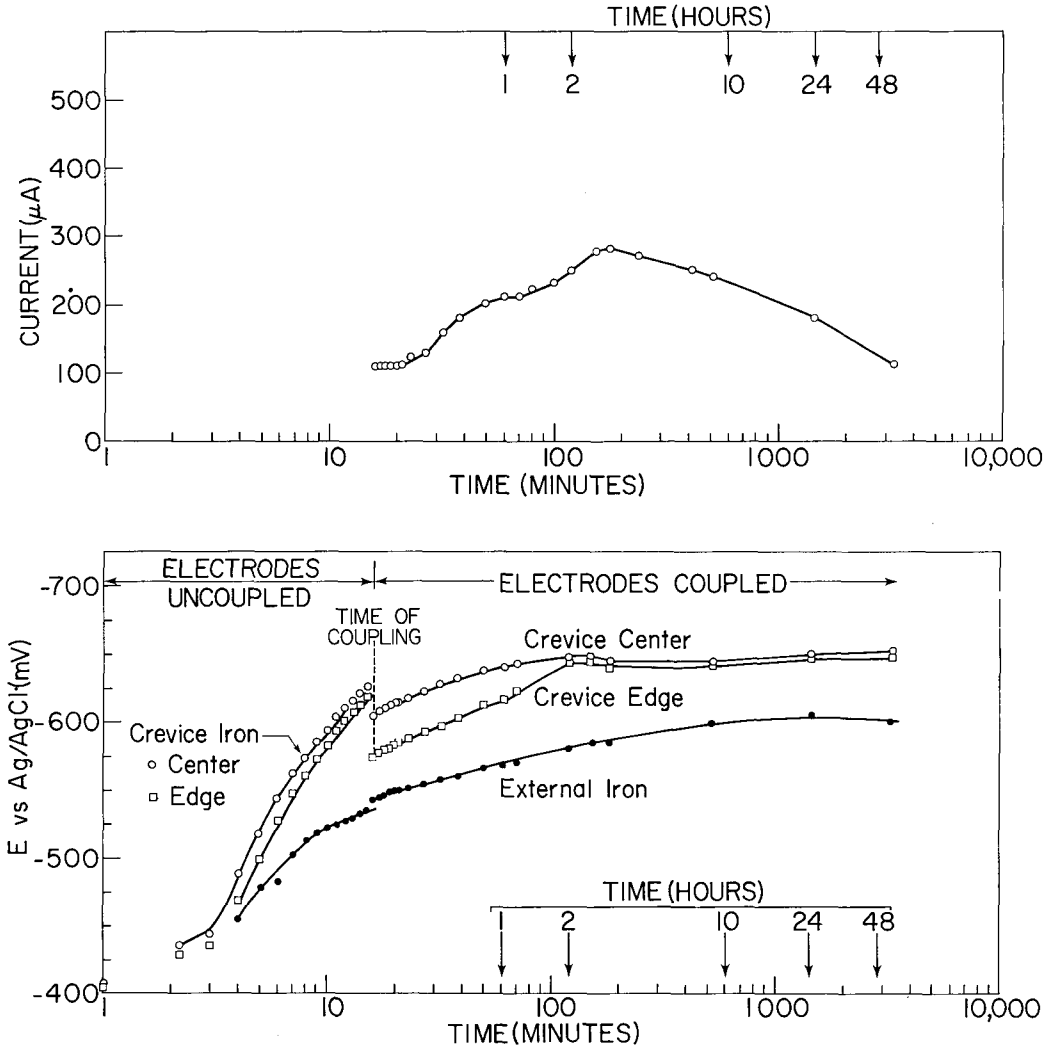

Fig. 16b — Effect of coupling iron within a 10-mil (0.25-mm) crevice in 0.006N Na_2CrO_4 + 0.06 NaCl to open external iron (area of crevice iron = 7.9 cm^2; area of external iron = 50 cm^2)

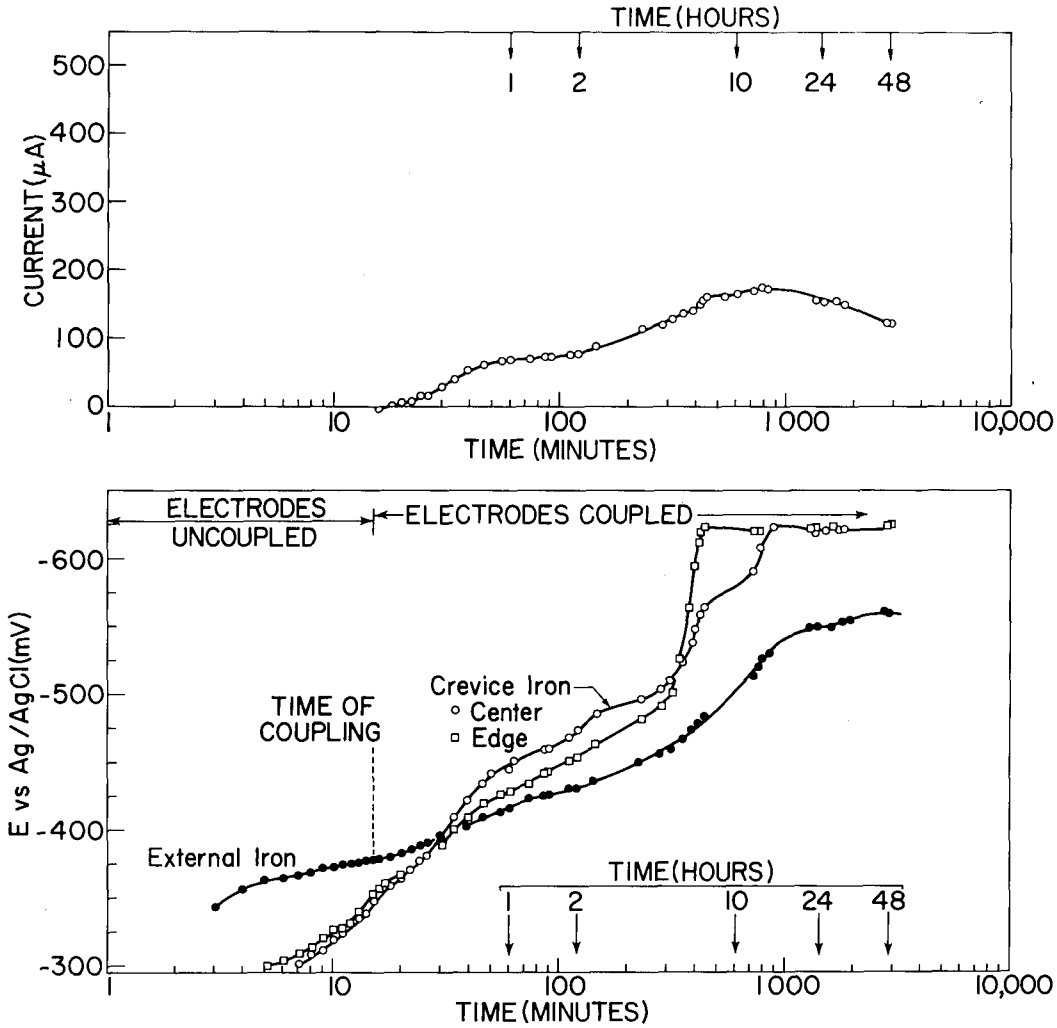

Fig. 16c — Effect of coupling iron within a 10-mil (0.25-mm) crevice in 0.006N Na_2CrO_4 + 0.006N NaCl to open external iron (area of crevice iron = 7.9 cm^2, area of external iron = 50 cm^2)

open iron in deaerated 1N chloride [37,38] (Fig. 17). If open iron in bulk solutions deaerated by intentional degassing is used as a scaled-up model for crevice iron in small volumes deaerated by oxygen consumption, then the anodic partial curve for crevice iron will intersect the cathodic curve for open iron at a decreased current. As shown in Figs. 16, the electrode potential of the crevice iron was essentially constant after the maximum in crevice corrosion current had been reached.

An increase in Cl^- content within the crevice, as predicted [10] or observed with artificial crevices [12,17,39,40] could also cause a decrease in anodic current, according to the "halide-inhibited" mechanism of iron dissolution [35]. Only if there is a drastic increase in Cl^- concentration (approximately 3M to 6M) *coupled* with an intense acidity

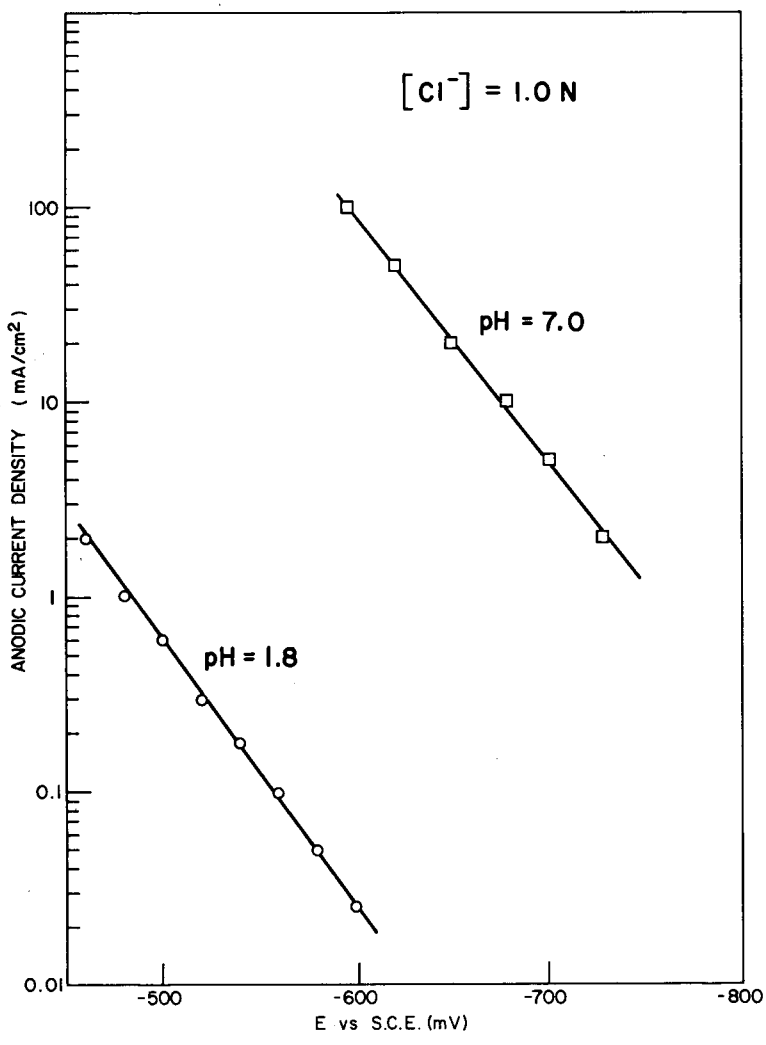

Fig. 17 — Effect of acidity on the anodic current density of iron in 1.0N chloride (data replotted from Nobe and coworkers [37, 38])

(pH < 0) will there be acceleration of the anodic reaction caused by the conjoint action of Cl^- and H^+ ions [36,41]. Figure 18 shows the anodic current for open iron as a function of acidity for a fixed chloride concentration of 6N.

In addition, insoluble corrosion products which accumulate within the crevice form a resistive barrier, which also serves to decrease the crevice corrosion current. For the experiment in Fig. 16a, gross bleeding of rust out of the crevice was first noticed at about 10 hours. All crevices which underwent corrosion were heavily laden with corrosion products after termination of the 48-hour runs.

The effect of the $CrO_4^=$ ion is seen in Fig. 19a, which shows the crevice corrosion current at a constant Cl^- concentration of 0.6N. The crevice corrosion current decreases

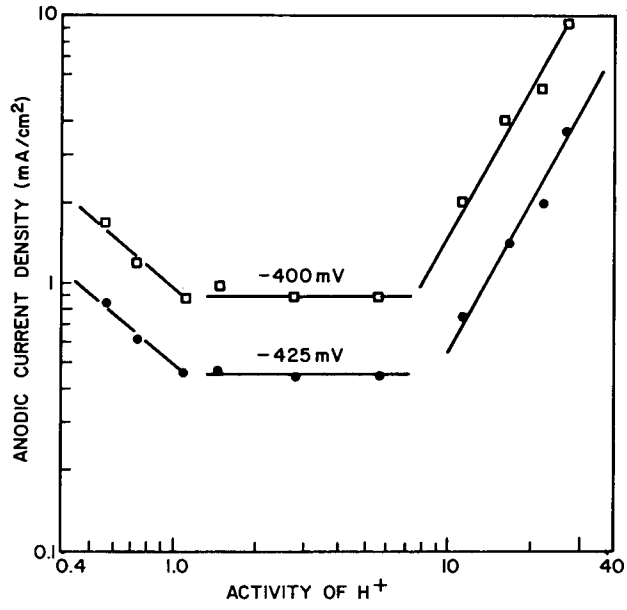

Fig. 18 — Effect of acidity on the anodic current density of iron in 6N chloride (McCafferty and Hackerman [33])

with increasing amounts of chromate inhibitor. Duplicate runs in Fig. 19a show that the trends are clear though the exact shapes of the curves are not identically reproducible.

Sodium chromate is an effective inhibitor of crevice corrosion if present in a sufficiently large concentration. The amount required appears to depend on the Cl^- concentration, as shown in Table 6. The minimum amount of $CrO_4^=$ required lies somewhere between 1 and 10 times the Cl^- concentration.

The effect of the Cl^- ion is shown in Fig. 19b, which plots the crevice corrosion current for a constant $CrO_4^=$ concentration of 0.006N. In the early stages of the process the corrosion current is greater the greater the Cl^- ion concentration. However at longer times all the crevices exhibit essentially the same rate. This suggests that the long-term crevice corrosion rate is controlled by the common local chemistry set up in each of the occluded cavities. In each case the band of rust around the crevice mouth serves to restrict exchange of the local and bulk electrolytes.

Potential Difference Between Inner and Outer Surfaces

Table 7 compares the electrode potentials between internal active iron and external passive iron when coupled in $CrO_4^=$ solutions. The potential of the crevice center was measured with the reference electrode within the crevice top (Fig. 2). The potential of the open, external iron was measured with a similar reference electrode outside the crevice.

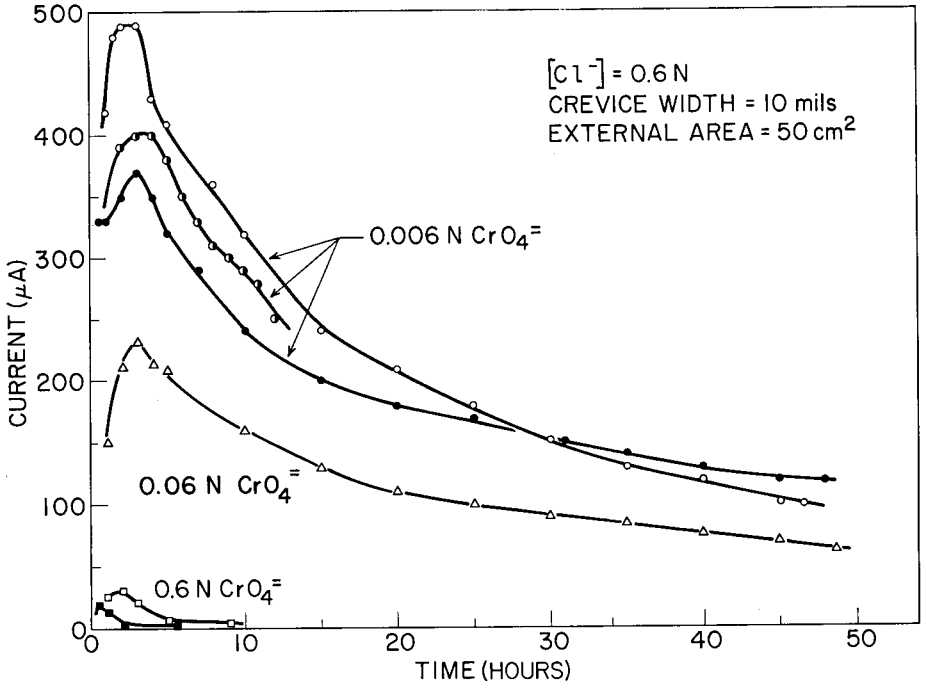

Fig. 19a — Effect of $CrO_4^{=}$ concentration on the crevice corrosion of iron at constant Cl^- concentration

Table 6
Inhibition of Crevice Corrosion by Sodium Chromate

$[Cl^-]$	Crevice Corrosion for Given $CrO_4^{=}$ Concentration?			Ratio of $[CrO_4^{=}]/[Cl^-]$ Which Gives Protection
	0.006N	0.06N	0.6N	
0.6N	Yes	Yes	No	1:1
0.06N	Yes	—	No	10:1
0.006N	Yes	No	—	10:1

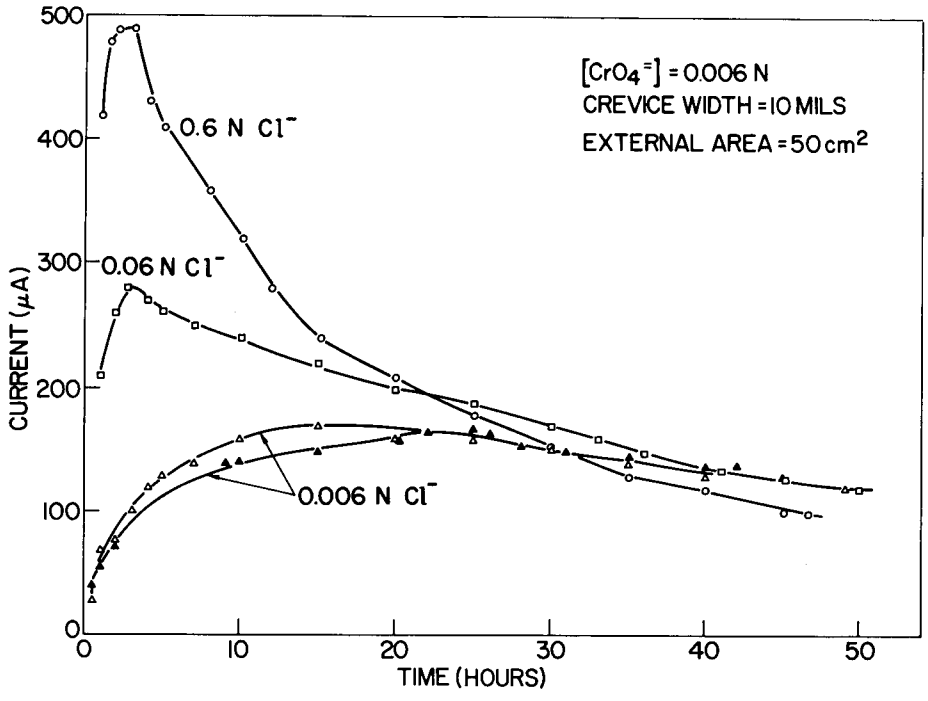

Fig. 19b — Effect of Cl^- concentration on the crevice corrosion of iron at constant $CrO_4^=$ concentration

Table 7
Potential Difference Between Crevice Center and Open Iron When Coupled

Conc. $CrO_4^=$ (N)	Conc. Cl^- (N)	Run. No.	$E_{external} - E_{crevice,\ center}$ (mV)						
			First Coupled	After 1 hr	After 6 hr	After 12 hr	After 24 hr	After 48 hr	Max ΔE
0.006	0.006	61	−21	28	63	87	71	58	99 (14 hr)
		78	22	74	100	105	106	87	106 (24 hr)
0.006	0.06	80	62	71	57	45	44	57	73 (7 hr)
0.006	0.6	60	26	29	15	11	9	7	34 (0.5 hr)
		76	17	25	16	14	—	—	30 (0.5 hr)
		79	5	17	17	—	14	17	21 (1.5 hr)
0.06	0.6	58	3	1	19	21	12	15	24 (4.5 hr)
0.6	0.6	57	13	14	14	11	5	—	14 (1 hr)
		66	3	3	4	1	—	—	5 (2 hr)

The electrode potential of the crevice was always more negative than that of the open metal (except for the first 30 minutes in Fig. 16c) due to a restricted oxygen supply to the crevice [3,4,9,42], but the potential difference between the two was fairly small: 10 to 100 mV for the active crevices (excluding the 0.6N Cl^-/0.6N $CrO_4^=$ solution, which showed little crevice corrosion). Data for repeat runs in Table 7 show the maximum potential difference between the crevice center and the open iron was reproducible to within 15 mV.

Steady-state potential differences between inner and outer stainless steel surfaces in 3-1/2% NaCl have been recently reported to be 50 to 150 mV [14,20]. According to Korovin and Ulanovskii [42], when the oxygen concentration in seawater is lowered from 9 to 1 mg/l, the change in potential of a 13% chromium steel coupled to platinum is shifted only 85 mV in the negative direction. This information as well as the data reported here shows that neither the initiation nor continuation of crevice corrosion requires a large potential difference between inner and outer metal surfaces. As noted by Karlberg and Wranglen [14], the concept of a large potential difference between the crevice and external metal is based on potential measurements of *uncoupled*, unpolarized components in solutions of differing oxygen content. As shown in Figs. 16, the potential difference between the inner and outer iron surface is much larger before coupling than after.

Potential Difference and Corrosion Rate

Figure 20 shows the crevice corrosion current as a function of potential difference between the crevice center and open, external iron. The data in the figure are for a fixed $CrO_4^=$ concentration of 0.006N with varying Cl^- content. In each case the open iron and crevice iron were coupled after 15 minutes, as in Figs. 16. The arrows in Fig. 20 show the direction of increasing time.

It can be seen that there is no simple relationship between the potential difference and the crevice corrosion rate over the entire process (48 hours). However the plots do exhibit some general features:

- Initially, each plot has a region in which the corrosion rate *increases* with increasing potential difference. This region was complete in 0.5 hour for 0.6N NaCl, 1.0 hour for 0.06N NaCl, and 2.5 hours for 0.006N NaCl. This region corresponds to initiation of crevice corrosion by oxygen depletion and passivity breakdown. Here the driving force for the corrosion reaction is the development of a potential difference between outer and inner metal by oxygen depletion within the crevice.

- The maximum crevice corrosion rate does not necessarily occur at the maximum potential difference. For 0.6N and 0.06N Cl^- the maximum corrosion rate occurred following a region in which the rate *increased* though the potential difference was *decreasing*. For 0.006N Cl^- however (and in a duplicate run) the maximum rate did occur at the maximum potential difference.

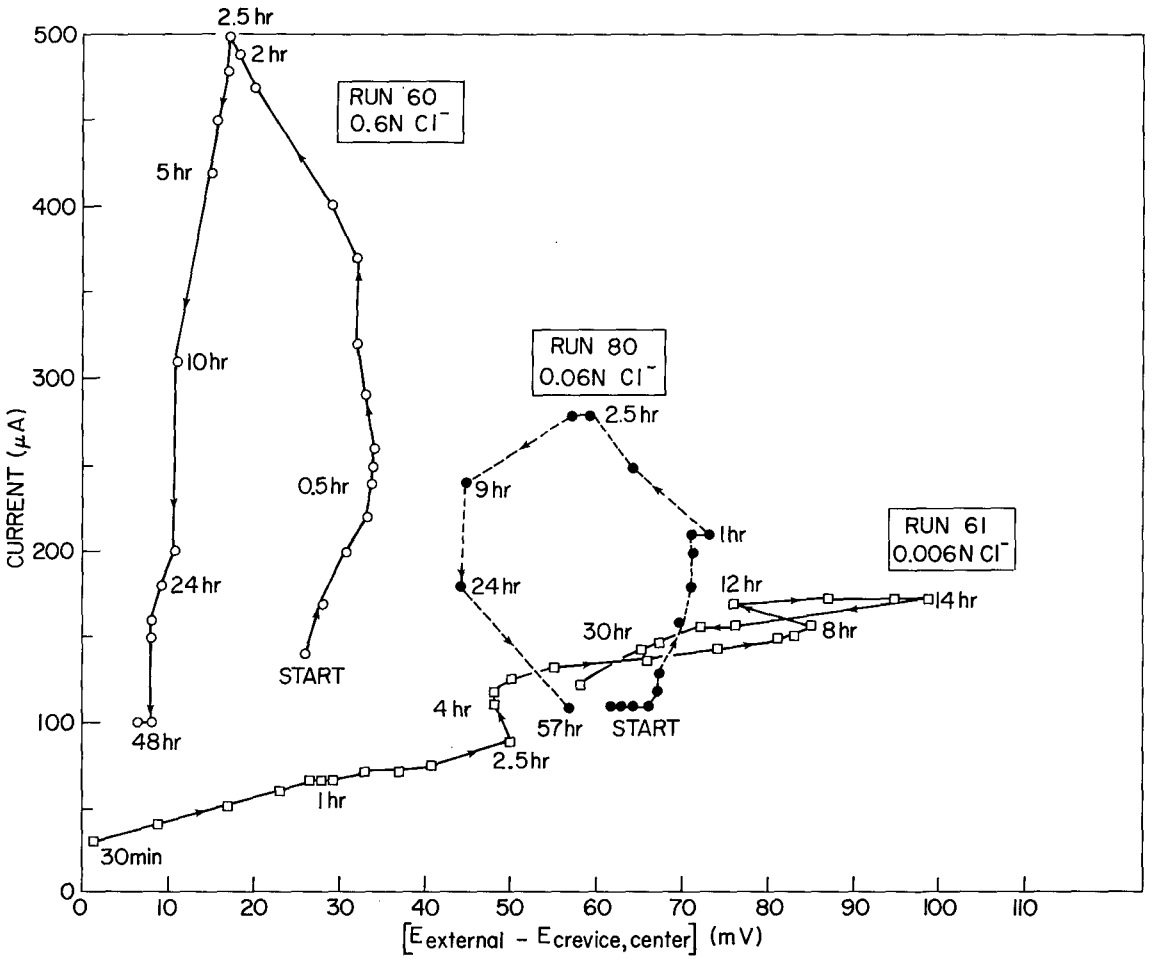

Fig. 20 — Sequential mapping of the potential difference between internal and external iron in 0.006N $CrO_4^{=}$ solutions (10-mil crevices)

- After the maximum crevice corrosion rate was reached, both the current and potential difference decreased with time. The decrease in current is caused by changes in the composition of the crevice and the appearance of resistive films, as discussed earlier.

Thus the potential difference between inner and outer parts which results due to oxygen depletion within the crevice is rate determining for the initiation, but not the propagation, of crevice corrosion.

Distribution of Crevice Attack

Attack in the crevice was not uniform. In all cases, attack was most severe around the edges of the iron surface near the crevice opening. This observation is consistent with

that of Karlberg and Wranglen [14], who noted that attack with 13% and 17% chromium steels always started near the mouth of the crevice. Preferential edge attack is also observed in many practical immersion tests [43].

A mathematical analysis of the distribution of current within a circular crevice has been completed. The current distribution was found to be a complicated function of crevice geometry and polarization behavior. For small crevice openings and appropriate polarization parameters the anodic current was calculated [44] to be largest near the crevice edges, as was observed experimentally. Details will be given elsewhere.

Comparison of Crevice Corrosion and Pitting

As discussed earlier, with ferrous metals stress-corrosion cracks, corrosion pits, and crevices all develop local internal acidities even when the bulk electrolyte is neutral or basic. In all three cases a special restrictive geometry produces an active local corrosion cell by limiting the exchange of the bulk and local electrolytes. In the case of pitting corrosion a porous cap of corrosion products acts as the barrier; within crevices and stress-corrosion cracks the long narrow diffusion path limits the access to bulk electrolyte. Thus the common features of restrictive geometry and local acidity have led to the point of view that all three forms of localized corrosion are different geometrical manifestations of the same general phenomenon of "occluded cell corrosion" [1]. That is, corrosion pits are *micro-crevices*, or crevices are *macro-pits*. However, though there are similarities, there also remain major *differences* between crevice corrosion and pitting.

Accordingly the pitting corrosion of iron was investigated in several of the $CrO_4^{=}/Cl^-$ solutions used in the crevice corrosion work. Pitting was studied by anodic polarization of the same iron electrode (7.9 cm^2) used in the crevice corrosion experiments except that the electrode was kept open to the solution. The open iron electrode was prepared as before and immersed in the solution until a steady-state open-circuit potential was established (usually 72 hours). The electrode potential of the open iron was measured with a chlorodized silver wire immersed directly in the solution near the electrode surface. The potential was adjusted to the Ag/AgCl standard electrode using the data from Fig. 4.

The anodic polarization curve for the open iron was then determined. Potentials were increased in the positive direction in discrete steps. In the absence of pitting, the current decreased to a steady value in 0.5 to 2 hours. But when pitting first occurred, the current increased steadily with time at that given potential. This potential at which pitting is first observed is called the *pitting potential*. At potentials above (more positive than) the pitting potential the current also increased with time.

Figure 21a shows anodic polarization curves for iron in 0.6N $CrO_4^{=}$ with varying amounts of Cl^- ion. Additions of 0.006N Cl^- and 0.06N Cl^- caused no pitting, and both solutions maintained passivity over the potential regions from open circuit to oxygen evolution. However with 0.6N Cl^- pitting started at a potential of −450 mV. The increase in current with time after the onset of pitting is shown by dashed lines which connect the initial current at a given potential with the value after 5 to 10 minutes at that same potential.

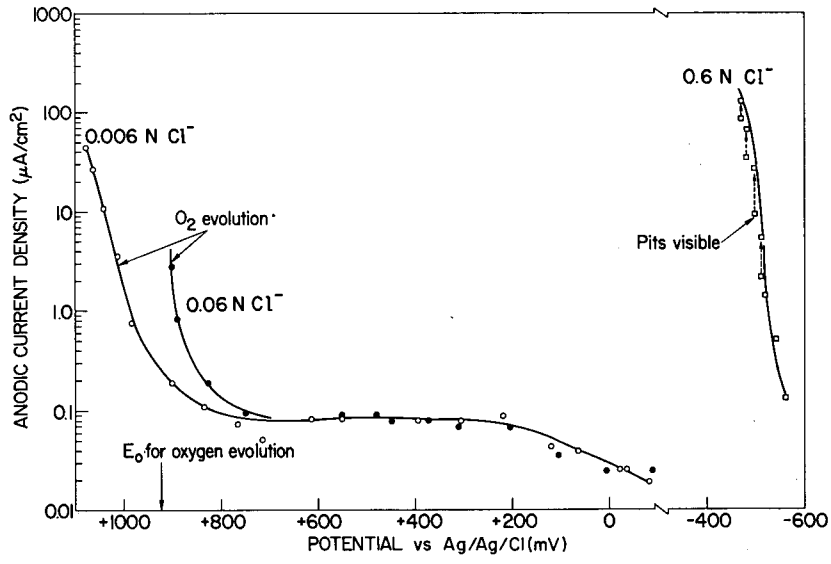

Fig. 21a — Anodic polarization of open iron in 0.6N $CrO_4^{=}$ for varying amounts of iron

Figure 21b shows similar pitting results for 0.006N $CrO_4^{=}$ solutions with varying amounts of Cl^- ion. The pitting potential is less positive for the higher Cl^- concentrations. That is, with increased Cl^- content, pitting occurs more easily, (at a less positive potential).

Uhlig [45] and Leckie and Uhlig [46] have demonstrated that the pitting potential is a well-defined electrochemical characteristic of a given system. At potentials below (less positive than) the pitting potential, pits do not initiate; but above the pitting potential, pits grow.

Table 8 compares some results from the pitting and crevice corrosion experiments. The table indicates that samples which pit when open do not necessarily undergo crevice corrosion when shielded. For example iron in 0.6N $CrO_4^{=}$ + 0.6N Cl^- readily pitted (Fig. 21a) but did not crevice corrode (Fig. 19a). The electrode potentials within the crevice was always less positive than the pitting potential, so that this comparison supports the idea that a crevice is a *macro-pit*. According to this view, crevice corrosion (*macro-pitting*) did not occur because the pitting potential was not surpassed. However, in the other two examples in Table 8, crevice corrosion occurred at potentials decidedly *less positive* than the pitting potential.

This difference in the electrode-potential behavior of pits and crevices emphasizes that the mechanism of passivity breakdown is different in the two cases. In the case of pitting, pit initiation is due to the adsorption of aggressive ions, such as Cl^-, which accumulate at increasingly positive potentials until at the pitting potential their concentration is sufficient to cause a local breakdown in passivity. With crevice corrosion however depletion of oxygen within the crevice and the development of local acidity causes the

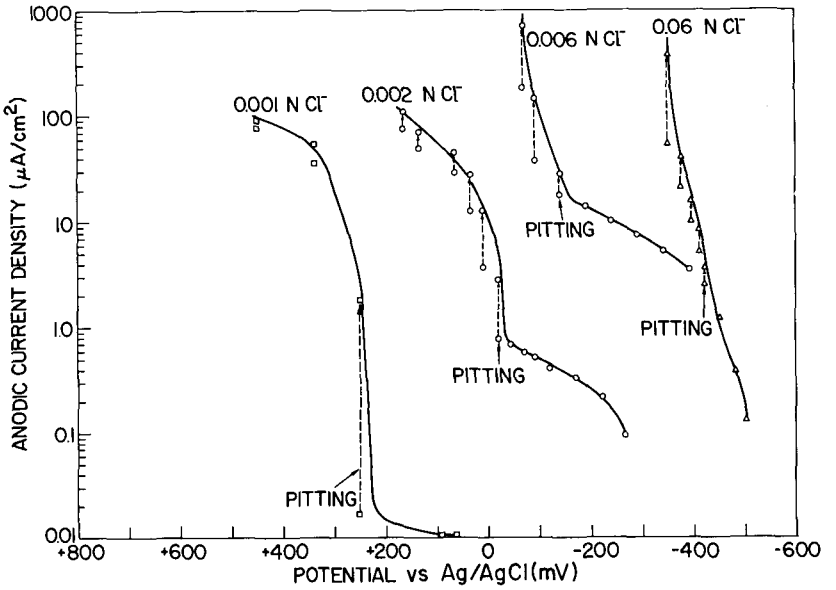

Fig. 21b — Anodic polarization of open iron in 0.006N $CrO_4^{=}$ for varying amounts of iron

Table 8
Comparison of Pitting Corrosion and Crevice Corrosion of Iron in $CrO_4^{=}/Cl^-$ Solutions

Example	Pitting Potential vs Ag/AgCl (mV)	Crevice Potential			
		Run	Location	Potential vs Ag/AgCl (mV)	
				At 0 hr	After Given Time
Pitting Corrosion on Open Iron; No Crevice Corrosion on Shielded Iron					
0.6N $CrO_4^{=}$ + 0.6N Cl^-	−450	57	Center	−450	−532 (28 hr)
			Edge	−446	−533 (28 hr)
		66	Center	−455	−526 (21 hr)
			Edge	−454	−527 (21 hr)
Pitting Corrosion on Open Iron; Crevice Corrosion on Shielded Iron					
0.006N $CrO_4^{=}$ + 0.006N Cl^-	−140	61	Center	−353	−621 (48 hr)
			Edge	−357	−624 (48 hr)
		78	Center	−372	−626 (44 hr)
			Edge	−413	−626 (44 hr)
0.006N $CrO_4^{=}$ + 0.06N Cl^-	−420	80	Center	−600	−653 (55 hr)
			Edge	−570	−650 (55 hr)

breakdown in passivity, without the necessity of Cl^- participation. Thus there appears to be no well-defined critical potential for crevice corrosion, and the internal electrode potential need not be related to the critical potential which causes pitting on open samples.

SUMMARY

For isolated crevices (internal iron not short-circuited to external iron):

- The anodic corrosion rate was determined by the limiting current for oxygen reduction.
- The limiting cathodic current, and hence the corrosion rate, was less than that for the open sample.
- For crevice heights less than the thickness of the oxygen diffusion layer the limiting cathodic current, and hence the corrosion rate, was suppressed to a constant value.
- The limiting cathodic current for oxygen reduction was not dependent on pH or Cl^- concentration.

For coupled crevices (internal iron short-circuited to external iron or platinum):

- The initial current increased with an increase in the Cl^- concentration or in the area of the external electrode but did not depend on the crevice height.
- In the $CrO_4^=/Cl^-$ solutions the crevice corrosion currents increased with time to maxima but then decreased.
- At constant Cl^- concentration the crevice corrosion current decreased with increasing $CrO_4^=$ concentration.
- At constant $CrO_4^=$ concentrations which are not protective the crevice corrosion current was greater the greater the Cl^- concentration for the early stages of the process, but at longer times the corrosion rates for all Cl^- concentrations were the same.
- Attack within the crevice was not uniform and was most severe near the crevice mouth.
- The electrode potential within the crevice is not related to the critical potential of pitting for the open sample.

ACKNOWLEDGMENT

This work was supported in full by the Office of Naval Research.

REFERENCES

1. B.F. Brown, Corrosion **26**, 249 (1970).
2. E. McCafferty, J. Electrochem. Soc. **121**, 1007 (1974).
3. I.L. Rosenfeld and I.K. Marshakov, Corrosion **20**, 115t (1964).
4. I.L. Rosenfeld and I.K. Marshakov, Zh. Fiz. Khim. **30**, 2724 (1956).
5. H.H. Uhlig, *Corrosion and Corrosion Control*, John Wiley, New York, 1971, p. 26.
6. M.H. Peterson, T.J. Lennox, Jr., and R.E. Groover, Materials Protection **9** (No. 1), 23 (1970).
7. B.F. Brown, C.T. Fujii, and E.P. Dahlberg, J. Electrochem. Soc. **116**, 218 (1969).
8. J.A. Smith, M.H. Peterson, and B.F. Brown, Corrosion **26**, 539 (1970).
9. M. Pourbaix, Corrosion **26**, 431 (1970).
10. M. Pourbaix, p. 17 in *The Theory of Stress Corrosion Cracking in Alloys*, J.C. Scully, editor, NATO, Brussels, 1971.
11. G. Butler, P. Stretton, and J.G. Beynon, Br. Corros. J. **7**, 168 (1972).
12. T. Suzuki, M. Yamabe, and Y. Kitamura, Corrosion **29**, 18 (1973).
13. F.D. Bogar and C.T. Fujii, "Solution Chemistry in Crevices on Fe-Cr Binary Alloys," NRL Report 7690, Mar. 1974.
14. G. Karlberg and G. Wranglen, Corrosion Sci. **11**, 499 (1971).
15. M.H. Peterson and T.J. Lennox, Jr., Corrosion **29**, 406 (1973).
16. B.E. Wilde and E. Williams, Electrochim. Acta 16, 1971 (1971).
17. Y. Kitamura and T. Suzuki, p. 716 in *Proceedings of the 4th International Congress on Metallic Corrosion*, Amsterdam, 1969, published by the National Association of Corrosion Engineers, 1972.
18. A. Pourbaix, Corrosion **27**, 449 (1971).
19. E.A. Lizlovs, J. Electrochem. Soc. **117**, 1335 (1970).
20. J.F. Bates, Corrosion, **29**, 28 (1973).
21. N.D. Greene, W.D. France, Jr., and B.E. Wilde, Corrosion **21**, 275 (1965).
22. D.J.G. Ives and G.J. Janz, editors, *Reference Electrodes*, Academic Press, New York, 1961, p. 205.
23. J. Dévay, B. Lengyel, Jr., and L. Meszáros, Acta Chimica Academiae Scientiarum Hungaricae **62**, 157 (1969).

24. Z.A. Iofa and M.A. Makhbuba, Protection of Metals (USSR) 3, 329 (1967).

25. G. Kar, I. Cornet, and D.W. Fuerstenau, J. Electrochem. Soc. 119, 33 (1972).

26. E.J. Kelly, J. Electrochem. Soc. 112, 124 (1965).

27. J.J. Lingane, *Electroanalytical Chemistry*, 2nd edition, Interscience, New York, 1958, p. 227.

28. "International Critical Tables," Vol. V, 1929, p. 64.

29. *Standard Methods for the Examination of Water and Wastewater*, 13th edition, American Public Health Association, Washington, D.C., 1971, p. 480.

30. I.L. Rozenfeld and O.I. Vashkov, Protection of Metals (USSR) 1, 56 (1965).

31. O.B. Ellis and F.L. LaQue, Corrosion 7, 362 (1951).

32. I.B. Ulanovskii and Yu.M. Korovin, J. Appl. Chem. (USSR), 35, 1683 (1962). [English translation of Zh. Prikl. Khim.]

33. I.B. Ulanovskii, J. Appl. Chem. (USSR), 39, 768 (1966). [English translation of Zh. Prikl. Khim.]

34. J.M. Fouts and C.W. Bergerson, Corrosion 13, 12t (1957).

35. W.J. Lorenz, Corrosion Sci. 5, 121 (1965).

36. E. McCafferty and N. Hackerman, J. Electrochem. Soc. 119, 999 (1972).

37. S. Asakura and K. Nobe, J. Electrochem. Soc. 118, 13 (1971).

38. R.J. Chin and K. Nobe, J. Electrochem. Soc. 119, 1457 (1972).

39. E.D. Parsons, H.H. Cudd, and H.L. Lochte, J. Phys. Chem. 45, 1339 (1941).

40. M.J. Pryor, Corrosion 9, 467 (1953).

41. N.A. Darwish, F. Hilbert, W.J. Lorenz, and H. Rossway, Electrochim. Acta 18, 421 (1973).

42. Yu.M. Korovin and I.B. Ulanovskii, Corrosion 22, 16 (1966).

43. K.D. Efird, International Nickel Co., Wrightsville Beach, N.C., personal communication, June, 1

44. E. McCafferty, Report of NRL Progress, Sept. 1973, pp. 66-69.

45. H.H. Uhlig, Materials Protection and Performance 12 (No. 2, Pt 1), 42 (1973).

46. H.P. Leckie and H.H. Uhlig, J. Electrochem. Soc. 113, 1262 (1966).